This is a preprint, the final version is subject to change, of the American Mineralogist (MSA)
Cite as Authors (Year) Title. American Mineralogist, in press.
(DOI will not work until issue is live.) DOI: http://dx.doi.org/10.2138/am-2017-5977

Revision 1

Rowleyite, $[Na(NH_4,K)_9Cl_4][V^{5+,4+}{}_2(P,As)O_8]_6 \cdot n[H_2O,Na,NH_4,K,Cl]$, a new mineral with a microporous framework structure

ANTHONY R. KAMPF[1§], MARK A. COOPER[2], BARBARA P. NASH[3], THURE E. CERLING[3], JOE MARTY[4], DANIEL R. HUMMER[5], AARON J. CELESTIAN[1], TIMOTHY P. ROSE[6], AND THOMAS J. TREBISKY[7]

[1]Mineral Sciences Department, Natural History Museum of Los Angeles County, 900 Exposition Boulevard, Los Angeles, CA 90007, USA

[2]Department of Geological Sciences, University of Manitoba, Winnipeg, Manitoba, R3T 2N2, Canada

[3]Department of Geology and Geophysics, University of Utah, Salt Lake City, Utah 84112, USA

[4]5199 East Silver Oak Road, Salt Lake City, UT 84108, USA

[5]Department of Geology, Southern Illinois University, Carbondale, IL 62901, USA

[6]Nuclear and Chemical Sciences Division, Lawrence Livermore National Laboratory, Livermore, CA 94550, USA

[7]MMT Observatory, University of Arizona, 1540 E. Second Street, Tucson, AZ 85721, USA

ABSTRACT

Rowleyite, $[Na(NH_4,K)_9Cl_4][V^{5+,4+}{}_2(P,As)O_8]_6 \cdot n[H_2O,Na,NH_4,K,Cl]$, is a new mineral species from the Rowley mine, Maricopa County, Arizona, U.S.A. It was found in an unusual low-temperature, apparently post-mining suite of phases that include a variety of vanadates, phosphates, oxalates, and chlorides, some containing NH_4^+. Other secondary minerals found in association with rowleyite are antipinite, fluorite, mimetite, mottramite, quartz, salammoniac, struvite, vanadinite, willemite, wulfenite, and several other potentially new minerals. Analyzed $\delta^{13}C$ values for the antipinite in association with rowleyite are consistent with a bat guano source. Crystals of rowleyite are very dark brownish green (appearing black) truncated octahedra up to about 50 μm in diameter. The streak is brownish green, the luster is vitreous, very thin fragments

§ Email: akampf@nhm.org

Always consult and cite the final, published document. See http:/www.minsocam.org or GeoscienceWorld

are transparent. The Mohs hardness is about 2, the tenacity is brittle, fracture is irregular, there is no cleavage, and the measured density is 2.23(2) g·cm^{-3}. Rowleyite is optically isotropic with n = 1.715(5). Electron microprobe analyses yielded the empirical formula $[(NH_4)_{8.81}Na_{3.54}K_{2.58})_{\Sigma 14.93}Cl_{6.29}(H_2O)_{16}][(V^{5+}_{9.36}V^{4+}_{2.64})_{\Sigma 12}(P_{5.28}As^{5+}_{0.72})_{\Sigma 6}O_{48}]$. Raman and infrared spectroscopy confirmed the presence of NH_4 and H_2O. Rowleyite is cubic, *Fd*-3*m*, with a = 31.704(14) Å, V = 31867(42) Å^3, and Z = 16. The crystal structure of rowleyite (R_1 = 0.040 for 1218 $F_o > 4\sigma F$ reflections) contains $[V_4O_{16}]^{12+}$ polyoxovanadate units that link to one another via shared vertices with $[(P,As)O_4]^{3-}$ tetrahedra to form a 3-D framework possessing large interconnected channels. The channels contain a 3-D ordered $[Na(NH_4,K)_9Cl_4]^{6+}$ salt net, which apparently served as a template for the formation of the framework. In that respect, rowleyite can be considered a salt-inclusion solid (SIS). The rowleyite framework is among the most porous known.

Keywords: rowleyite; new mineral species; polyoxovanadate; microporous framework; salt-inclusion solid; crystal structure; Rowley mine, Arizona.

INTRODUCTION

The Rowley mine, about 100 km southwest of Phoenix, Arizona, USA, is an old Cu-Pb-Au-Ag-Mo-V-baryte-fluorspar mine, which hasn't been worked for ore since 1923. Mineral collectors first took notice of the mine as a source of fine wulfenite crystals around 1945. In early 2013, one of the authors (TJT) found ammineite, $CuCl_2(NH_3)_2$, in the vicinity of bat guano at the end of the tunnel on the 125-foot level. A short time later, another of the authors (JM) discovered unusual mineralization 10 to 15 meters up the tunnel from the ammineite occurrence. His

Always consult and cite the final, published document. See http:/www.minsocam.org or GeoscienceWorld

attention was initially drawn to bluish-green specks that proved to be antipinite, $KNa_3Cu_2(C_2O_4)_4$. Both ammineite and antipinite are recently described species from the sea-bird guano deposit at Pabellón de Pica, Chile (Bojar et al., 2010; Chukanov et al., 2015). The suite of phases associated with the antipinite in the Rowley mine includes a remarkable assortment of vanadates, phosphates, oxalates, and chlorides, some of which contain NH_4^+, and many of which are new. Herein, we describe the first of these new phases, rowleyite, which is named for the locality, the Rowley mine. The polyoxometalate framework structure of rowleyite is noteworthy for being among the most porous known.

The new mineral and name were approved by the Commission on New Minerals, Nomenclature and Classification of the International Mineralogical Association (IMA 2016-037). Five cotype specimens of rowleyite are deposited in the collections of the Natural History Museum of Los Angeles County, Los Angeles, California, USA, catalogue numbers 66268, 66269, 66270, 66271, and 66272.

OCCURRENCE

Rowleyite was found on the 125-foot level of the Rowley mine, Theba, Painted Rock district, Maricopa County, Arizona, USA (33°2'57"N 113°1'49.59"W). The Rowley mine is a former Cu-Pb-Au-Ag-Mo-V-baryte-fluorspar mine that exploited veins presumed to be related to the intrusion of an andesite porphyry dike into Tertiary volcanic rocks. The most detailed recent account of the history, geology, and mineralogy of the mine was by Wilson and Miller (1974).

The new mineral was found in an unusual low-temperature, apparently post-mining suite of phases that include a variety of vanadates, phosphates, oxalates, and chlorides, some containing NH_4^+. This secondary mineral suite is found growing on baryte-rich matrix and,

Always consult and cite the final, published document. See http:/www.minsocam.org or GeoscienceWorld

besides rowleyite includes antipinite, fluorite, mimetite, mottramite, quartz, salammoniac, struvite, vanadinite, willemite, wulfenite, and several other potentially new minerals. This area of the mine is generally hot and humid. While no bat guano is observed in close proximity to the suite containing rowleyite, 10 to 15 meters further down the tunnel is an area encrusted with bat guano in the proximity of which ammineite has been found.

It seems most likely that the source of the ammonium, oxalate, and phosphate in the phases of this unusual suite is an earlier bat guano encrustation (cf. Snow et al., 2014). Other possibilities that we considered were decomposing saguaro cactus (*Carnegiea gigantea*) on the surface above the mine and decomposed dynamite left from the earlier mining activities. To better assess these possibilities, we conducted a carbon isotope analysis of crystals of antipinite from this mineral assemblage. In particular, it is important to distinguish a dynamite source from natural sources, since an anthropogenic source of material would influence rowleyite's categorization as a mineral species. As rowleyite lacks carbon, associated crystals of antipinite were used for analysis.

Purified grains of the antipinite were analyzed using an elemental analyzer (EA) coupled to an isotope ratio mass spectrometer (IRMS). Five replicate analyses were performed on samples ranging from 31 to 44 μg; the low sample masses reflect the small grain size and relative rarity of the phase. The average $\delta^{13}C$ value for the five analyses is -18.0 ± 0.5 permil VPDB. The measured carbon content was 18± 2%, which is consistent with the calculated carbon content of 16.3% to within the uncertainty of the analyses.

The calcium oxalate whewellite has been reported from a number of hydrothermal vein systems with a range in $\delta^{13}C$ values that overlaps with those of the Rowley mine antipinite (Hofmann and Bernasconi, 1998); however, hydrothermal oxalates were not previously reported

Always consult and cite the final, published document. See http:/www.minsocam.org or GeoscienceWorld

in the Rowley vein despite extensive mineralogical investigations (e.g. Wilson and Miller, 1974).

Old dynamite formulations used ammonium oxalate as an additive (Thorpe, 1922). The ammonium oxalate was likely produced from oxalic acid, which was historically manufactured by treating sawdust with a strong caustic solution (Von Wagner, 1900). Sawdust from plants that use the C3 photosynthetic pathway have $\delta^{13}C$ values that range from -23 to -35 permil with an average near -26 (O'Leary, 1988). If the Rowley mine antipinite was derived from the residue of deteriorated dynamite, it would require a carbon isotope fractionation process that could drive the $\delta^{13}C$ values toward more ^{13}C-enriched values.

Rivera and Smith (1979) analyzed calcium oxalates from five different cacti species and observed a narrow range in $\delta^{13}C$ values between -7.3 and -8.7 permil. Carbon isotope analyses of biomineralization associated with decomposing saguaro cactus in southern Arizona are consistent with this range in values (Garvie, 2003). These reported oxalate $\delta^{13}C$ values from cacti have a carbon isotope signature that is distinct from that of the Rowley mine antipinite.

Bat guano from caves has been observed to have oxalate minerals associated with it (Frost et al., 2008; Mercè Bergadà, 2013). Stable isotope studies of bats from the southwestern USA have been shown to have $\delta^{13}C$ values ranging from C_3-dominated to C_4/CAM dominated (O'Leary, 1988), with diets ranging from *ca*. -10 to -25‰ (Des Marais et al., 1980; Fleming et al. 1993; Wurster et al., 2007), spanning the observed range of $\delta^{13}C$ in the Rowley mine antipinite. Thus, the analyzed $\delta^{13}C$ values for the antipinite in association with rowleyite are most consistent with a bat guano source.

PHYSICAL AND OPTICAL PROPERTIES

Crystals of rowleyite are truncated octahedra, up to about 50 μm in diameter, and

Always consult and cite the final, published document. See http:/www.minsocam.org or GeoscienceWorld

exhibiting the forms {100} and {111}, up to about 0.1 mm in diameter (Fig. 1). Intergrowths of interpenetrant crystals are common, but no twin law could be ascertained. The megascopic color is very dark brownish green, appearing black; in transmitted light, an olive-green rim is observed to surround a red-brown core. The luster is vitreous and crystals are transparent in very thin fragments. The streak is brownish green. Rowleyite is non-fluorescent in long- and short-wave ultraviolet light. It has a Mohs hardness of about 2, brittle tenacity, irregular fracture, and no cleavage. The density measured by floatation in a mixture of methylene iodide and toluene is 2.23(2) $g \cdot cm^{-3}$. The calculated density is 2.04 $g \cdot cm^{-3}$ using the empirical formula for 16 H_2O *pfu*; 2.28 $g \cdot cm^{-3}$ using the empirical formula for 32 H_2O *pfu*. The mineral is insoluble in H_2O at room temperature. In dilute HCl, it immediately turns orange and slowly dissolves.

Rowleyite is optically isotropic with $n = 1.715(5)$ measured in white light. Note that the determination of the index of refraction was problematic because different portions of crystal fragments provided very different readings. The value reported is for uniformly olive-green outer rims; however, more fractured red-brown cores had a much lower index of refraction, which was difficult to measure.

RAMAN SPECTROSCOPY

Raman spectroscopy was conducted on a Thermo Nicolet Almega micro-Raman spectrometer at the Department of Geoscience, University of Arizona. An equant, ~30 μm crystal of rowleyite was measured using an incident wavelength of 532 nm and a laser aperture of 25 μm. Because rowleyite was apparently susceptible to burning by the beam due to the ~2 μm spot size, data was collected for ~2 hrs at a reduced laser power of 5.0 mW, which achieved sufficient signal-to-noise ratio without altering the spectrum during data collection.

Always consult and cite the final, published document. See http:/www.minsocam.org or GeoscienceWorld

The Raman spectrum of rowleyite is shown in Figure 2. Bands centered on ~830 and ~1000 cm^{-1} were assigned to V–O and P–O lattice stretches, respectively (Frost et al. 2011, 2015). The much stronger intensity of the V–O band is consistent with our microprobe measurements showing more than twice as much V as P on a molar basis. The V–O band in rowleyite is centered at the lower end of the typical 820–900 cm^{-1} frequency range for V–O stretching modes in vanadates with VO_4 tetrahedra (Frost et al. 2011), as well as the very similar 822-973 cm^{-1} frequency range for minerals such as cavansite and pentagonite that, like rowleyite, also contain VO_5 groups (Frost and Xi, 2012). Three distinct bands centered at ~180, 280, and 330 cm^{-1} represent vibrations of the entire lattice.

INFRARED SPECTROSCOPY

Infrared spectroscopy was conducted on a Jasco IMV-4000 Infrared Multichannel spectrometer at the Geophysical Laboratory, Carnegie Institution for Science. An equant rowleyite crystal with diameter ~30 μm was measured using a halogen lamp with an aperture of 50 μm to encompass the entire crystal for minimum background noise. Data was collected for ~6 min at a resolution of 8 cm^{-1}, and the experimental spectrum was normalized to a blank spectrum collected at identical conditions to remove strong absorption lines from atmospheric gases.

The IR spectrum of rowleyite is shown in Figure 3. A suite of overlapping bands occurs in the 2600–3400 cm^{-1} range, typical of N–H stretching modes (Pankewitz et al. 2007). A shoulder at ~3600 cm^{-1}, significantly higher frequency than any N–H vibration, can only be due to O–H stretching and confirms that rowleyite is hydrous. The presence of a 3600 cm^{-1} band can be due to a variety of O- and H-bearing molecular species, but because our structural analysis suggests the presence of significant structural H_2O in the channels of rowleyite (and because of

Always consult and cite the final, published document. See http:/www.minsocam.org or GeoscienceWorld

the presence of the band discussed below), we propose that molecular H_2O is the most logical assignment for the 3600 cm^{-1} band. Due to the strong overlap between these high frequency bands, however, it is difficult to assign precise peak positions and postulate distinct structural sites for the H_2O and NH_4^+. A strong band centered at ~1600 cm^{-1} is assigned to a combination of O–H and N–H bending modes (Varriale et al. 2011), and a weak band at 1900–2000 cm^{-1} could not be assigned to any obvious feature of the rowleyite structure. Below 1500 cm^{-1}, the instrument registered very low transmitted intensity in both the sample and blank spectra, and therefore the normalized spectrum contains only random noise in this region.

CHEMICAL ANALYSIS

Analyses of rowleyite (5 points over 3 crystals) were performed at the University of Utah on a Cameca SX-50 electron microprobe with four wavelength dispersive spectrometers utilizing Probe for EPMA software. Analytical conditions were 15 keV accelerating voltage, 10 nA beam current, and a beam diameter of 10 μm. Counting times were 20 seconds on peak and 20 seconds on background for each element, except N for which 40 second counting times were used. Raw X-ray intensities were corrected for matrix effects with a $\phi\rho(z)$ algorithm (Pouchou and Pichoir, 1991). Significant damage from the electron beam was observed. Time-dependent intensity corrections were applied to the Na, K, and V analyses. The sensitivity of rowleyite to the electron beam precluded the use of area peak ratios in the determination of nitrogen because of the long counting times that would be required to acquire the spectra. Accordingly, peak intensity ratios were used following the methodology as described by Bastin and Heijligers (1991). The primary standard was synthetic Cr_2N with secondary standards of GaN and HfN.

Always consult and cite the final, published document. See http:/www.minsocam.org or GeoscienceWorld

Because of the thinness of the olive green rims, the analyses were conducted principally on the red-brown crystal cores, which appear to be significantly higher in P and lower in V than the rim, on which the structure refinement was conducted. H_2O was not analysed because of paucity of material. Analytical data are given in Table 1.

As noted below in the discussion of the crystal structure, the open porous structure of rowleyite with highly mobile channel constituents means that the electron-microprobe results must be regarded as a semi-quantitative approximation of the composition. The structure determination provides a better indication of the composition, so we have used a combination of EPMA and structural evidence to propose empirical formulas consistent with three different possible channel contents (see structure discussion below).

As shown in column 2 of Table 2, the empirical formula (based on 18 P+V+As and with 16 H_2O *pfu*) is $[(NH_4)_{8.81}Na_{3.54}K_{2.58})_{\Sigma 14.93}Cl_{6.29}(H_2O)_{16}][(V^{5+}_{9.36}V^{4+}_{2.64})_{\Sigma 12}(P_{5.28}As^{5+}_{0.72})_{\Sigma 6}O_{48}]$. The simplified structural formula is $[Na(NH_4,K)_9Cl_4][V^{5+,4+}_2(P,As)O_8]_6 \cdot n[H_2O,Na,NH_4,K,Cl]$. The Gladstone-Dale compatibility (Mandarino, 2007) $1 - (K_p/K_c)$ is -0.166 (poor) for 16 H_2O *pfu* and 0.029 (excellent) for 32 H_2O *pfu*.

X-RAY CRYSTALLOGRAPHY AND STRUCTURE DETERMINATION

Powder X-ray studies were carried out using a Rigaku R-Axis Rapid II curved imaging plate microdiffractometer with monochromatized Mo$K\alpha$ radiation. A Gandolfi-like motion on the φ and ω axes was used to randomize the sample. Observed *d*-values and intensities were derived by profile fitting using JADE 2010 software (Materials Data, Inc.). Because of the difficulty in separating a pure sample, all recorded powder diffraction patterns exhibited extra peaks and/or some observed peaks of significantly greater intensity than the corresponding calculated peaks.

Always consult and cite the final, published document. See http:/www.minsocam.org or GeoscienceWorld

This may also reflect structural differences between the olive-green crystal rims (used for the structure determination) and the red-brown crystal cores. The powder data are presented in Table 3. Unit-cell parameters refined from the powder data using JADE 2010 with whole pattern fitting are: a = 31.73(2) Å and V = 31946(60) Å^3.

Single-crystal X-ray studies were carried out on an olive-green fragment removed from the rim of a crystal. The complete Ewald sphere of data (including some duplicates) was collected using 60s per 0.3° frame with a crystal-detector distance of 5 cm. The unit-cell dimensions were obtained by least-squares refinement of 4095 reflections with $I > 10\sigma I$. A total of 236208 reflections were integrated. Systematically absent reflections are consistent with the space group *Fd*-3*m*. Empirical absorption corrections (SADABS; Sheldrick, 2015) were applied and equivalent reflections were merged. The structure was solved by direct methods using SHELXS-2013 and the structure was refined using SHELXL-2013 (Sheldrick, 2015). Data collection and refinement details are given in Table 4, atom coordinates and displacement parameters in Table 5, selected bond distances in Table 6, site assignments in Table 7, and a bond-valence analysis in Table 8.

DISCUSSION

Site assignments in the framework

The crystal structure of rowleyite contains two V sites that are fully occupied by dominant V^{5+} and subordinate V^{4+} in a disordered fashion. Each V site is coordinated by five O atoms in a square pyramidal coordination. There is a short vanadyl (V=O) bond (~1.6 Å) to the apical oxygen and four longer equatorial bonds (~1.8–2.0 Å) to basal oxygens of the pyramid, otherwise referred to as a [1+4] coordination; this coordination environment is common for both $V^{5+}O_5$ and

Always consult and cite the final, published document. See http:/www.minsocam.org or GeoscienceWorld

235 $V^{4+}O_5$ polyhedra. An estimate of the average valence of V can be derived for a VO_5 polyhedron
236 from its average equatorial bond distance (*R*) using the equation <*Z*> = 25.99 – 11.11(*R*) in
237 mixed-valent structures (Schindler *et al*., 2000). In rowleyite, <V1–O_{eq}> = 1.910 Å and <V2–
238 O_{eq}> = 1.907 Å, and the average V valences are 4.77 and 4.80 *vu*, respectively, indicating a
239 strong dominance of V^{5+} over V^{4+} at both sites, and a high degree of V^{5+} – V^{4+} disorder between
240 the two sites. There is a single P site tetrahedrally coordinated by four O atoms; the refined
241 electron scattering at this site is in excess of 15 electrons [*i.e*. 17.16(9) *e*] and the observed <P–
242 O> distance of 1.557 Å is slightly greater than the anticipated 1.54 Å value from the added
243 respective radii ($^{IV}P^{5+}$ = 0.17, O = 1.37 Å; Shannon, 1976). A small amount of As was
244 encountered during electron-microprobe analysis (4.07 wt.% As_2O_5), and is assigned to the P site
245 to account for the excess size and electron density observed there. Site-occupancy refinement at
246 the P site utilizing the P and As scattering factors gives a P site composition of ($P_{0.88}As_{0.12}$) and a
247 calculated mean bond length of 1.560 Å, in close agreement with the observed value.
248
249 *Site-assignments in the channels*
250 The observed electron scattering in the channels displays a range of character from
251 reasonably small and uniform anisotropic displacement parameters to very large and varied
252 values, suggesting reasonably well-ordered (positionally) constituents along with very disordered
253 and possibly *mobile* constituents. Centered around the channel position at (1/8, 1/8, 1/8) is a
254 complex salt cluster comprised of two *A* sites and two Cl sites (Figure 4). The *A* sites are inferred
255 to be occupied by 75% NH_4^+ and 25% K^+ ions (via K/N site-occupancy refinement), and the Cl
256 sites by Cl. The *A*1 site is coordinated by nine O atoms and two Cl atoms with <*A*1–φ> = 3.147 Å
257 and the *A*2 site is coordinated by four O atoms and four Cl atoms with <*A*2–φ> = 3.167 Å. In the

Always consult and cite the final, published document. See http:/www.minsocam.org or GeoscienceWorld

structure of lucabindiite, the *M* site coordinated by twelve O atoms has an observed <*M*–O> distance of 3.127 Å and is occupied by $K_{0.51}(NH_4)_{0.49}$; this is in general agreement with the observed <*A*–O> distances in rowleyite and the observation that K^+ and NH_4^+ have similar ionic radii (Garavelli *et al*., 2013, Holleman & Wiberg, 2001). The bond valence analysis reveals that these channel cations (NH_4^+, K^+, Na^+) all contribute small, but significant, valence contributions to the O atoms of the surrounding vanadium-phosphate framework. The Cl3 site is positioned ~3 Å from the V1 and V2 sites in a *trans* position relative to the short vanadyl bond. The refined site-scattering at the Cl3 site of 13.0(2) electrons is in agreement with a Cl dominant site that is inferred to be occupied by ($Cl_{2.29}\square_{0.71}$) *pfu* [*i.e.* occupation at the nearby *X*6 and *X*7 sites necessitates complimentary vacancy at Cl3]. Additionally, there are twelve channel *X* sites that show highly varied occupancy and displacement character. The *X* sites electron density were included in the structural model to help constrain a lower limit to the total channel content; we recognize that additional highly mobile channel constituents absent in our structural model may also be present in rowleyite.

Description of the structure

The VO_5 square pyramids link at their bases (*via* corner-sharing) to form $[V_4O_{16}]$ units (Figure 5), and the remaining basal oxygens of the square pyramids interconnect to other $[V_4O_{16}]$ units via shared vertices with $[(P,As)O_4]$ tetrahedra (Figure 6) to form a 3-D framework possessing large interconnected channels (Figs. 7 and 8).

Centered at the channel position (1/8, 1/8, 1/8) in the rowleyite structure is the $[A_9Cl_4]^{5+}$ {actually $[(A_9Cl_4)_2]^{10+}$} salt cluster with the composition $[(NH_4)_{6.74}K_{2.26}Cl_4]$ *pfu* (Figs. 4 and 9). The Cl atoms are positioned at the corners of a cube; distances from the center position

Always consult and cite the final, published document. See http:/www.minsocam.org or GeoscienceWorld

(1/8,1/8,1/8) to Cl1 and Cl2 are 3.71 and 3.51 Å, respectively, and no significant electron density is located at the (1/8,1/8,1/8) position. The *A*2 sites are positioned at the vertices of an octahedron lying outside each of the faces of the inner Cl cube. The outer *A*1 sites are positioned at the vertices of a 14-faced polygon comprised of the forms cube + octahedron, with the faces of each form parallel to the inner Cl-cube and *A*2-octahedron forms, respectively. These $[A_9Cl_4]^{5+}$ salt clusters link tetrahedrally to four more such clusters through Na^+ ions (positioned over the octahedral faces of the 14-faced polygon that have Cl1 atoms lying below) along the channels to form a 3-D ordered $[Na(NH_4,K)_9Cl_4]$ salt net that carries a 6+ charge *pfu*. The twelve *X* sites represent approximate electron-scattering values and positions for the channel occupants (*i.e.* NH_4, K, Na, Cl, H_2O). Assigning specific atomic identity to these sites is problematic considering: the large number of *X* sites, their partial occupations, and highly variable degree of positional uncertainty (which includes numerous close approaches preventing mutual occupation). From the bond valence analysis of the ordered portion of the structure (Table 8), it is apparent that the anions O1, O2, and O4 remain slightly underbonded, and some of the *X* sites are expected to provide additional bond valence to these anions. We have listed all of the closer O–*X* distances in Table 6, and not surprisingly, all involve *X* sites that are proximal to these anions (*i.e.* O1, O2, O4).

Rowleyite belongs to the polyoxometalate (POM) group of chemical compounds, and more specifically, it contains $[V_4O_{16}]$ polyoxovanadate (POV) units. The synthetic compound $Cs_{3.64}Na_{1.40}(V_4O_8)(AsO_4)_2Cl_{3.04}$ is the closest structural synthetic POV to rowleyite (Queen *et al*., 2010). In this synthetic, all V is pentavelent. The $[V_4O_{16}]$ units are linked similarly by AsO_4 tetrahedra to form a $[V_2AsO_8]$ framework, which is topologically equivalent to that in rowleyite. Rowleyite can also be considered a phosphovanadate with a zeolite-like framework structure.

Always consult and cite the final, published document. See http:/www.minsocam.org or GeoscienceWorld

Among minerals, rowleyite is most similar to phosphovanadylite-Ba and phosphovanadylite-Ca, $(Ba,Ca)[P_2(V,Al)_4(O,OH)_{16}]\cdot 12(H_2O)$ (Kampf *et al*., 2013), which also are phosphovanadates with a zeolite-like framework structure; however, the phosphovanadylite structure has a very different linkage of VO_6 octahedra.

Framework porosity

The rowleyite framework is among the most porous known. It contains two types of cages (Figure 10). A small cage centered at 1/8, 1/8, 1/8 hosts the $[A_9Cl_4]^{5+}$ salt cluster and a large cage centered at 3/8, 3/8, 3/8 hosts the *X* sites. A measure of the porosity is the framework density, defined as the total number of regular polyhedra (tetrahedra, octahedra, and square pyramids) per 1,000 $Å^3$. Rowleyite has a framework density of 9.8 polyhedra/1000 $Å^3$, which we believe is the lowest of any naturally occurring crystalline framework material. By comparison, tschörtnerite (Baerlocher, 2007) with a framework density of 12.1 has the lowest framework density of all natural zeolites, and traskite (Malinovskii *et al*., 1976) with a framework density of 11.7 has the lowest framework density of all natural heterosilicates. Phosphovanadylite-Ba and phosphovanadylite-Ca (Kampf *et al*., 2013), other minerals with a phosphate-vanadate framework, have a framework density of 13. Among synthetic materials, we are only aware of one type of compound with a lower framework density, the chalcogenide zeolite analog UCR-20 with a decorated sodalite-type structure (and its related structures UCR-21, 22, and 23; Zheng, *et al*. 2002), which have framework densities of 4.6 polyhedra/1000 $Å^3$.

In the rowleyite structure, the large cages are connected via a 12-membered ring with a diameter of 9.7 Å, and the large and small cages are also connected via a 12-membered ring, but

Always consult and cite the final, published document. See http:/www.minsocam.org or GeoscienceWorld

326 the apical oxygens of three VO_5 square pyramids point into this 12-membered ring, thus limiting
327 its effective ring diameter to 4.1 Å.
328
329 *Chemical formula based on the structure determination*
330 The average V valence of 4.78 *vu* derived from the average V–O_{eq} distances (Schindler *et*
331 *al*., 2000), and P/As ratio derived from site-occupancy refinement, gives
332 $[(V^{5+}_{9.36}V^{4+}_{2.64})_{\Sigma 12}(P_{5.28}As_{0.72})_{\Sigma 6}O_{48}]$ *pfu* for the rowleyite framework, which carries a net charge
333 of 8.64– *pfu*. The ordered channel $[Na(NH_4,K)_9Cl_4]$ salt component carries a 6+ charge *pfu*. The
334 Cl3 site gives a refined occupancy consistent with $(Cl_{2.29}\square_{0.71})$ *pfu* and provides a 2.29– charge.
335 Summing these constituent charge contributions leaves 4.93– to be balanced by the various *X* site
336 constituents. We can infer a lower limit to the total occupation of the channels using the total
337 refined site-scattering from the structure refinement, and couple this with an estimated relative
338 proportioning of the various *X* site occupants from the electron-microprobe results. In the case of
339 rowleyite (an open porous structure with mobile channel constituents), the electron-microprobe
340 results must be regarded as a semi-quantitative approximation of the chemistry –the sample was
341 subjected to high vacuum, and then punished under the electron beam; rowleyite before and
342 during electron-microprobe analysis are surely differing compounds with respect to channel
343 content within the analytical volumes investigated. In contrast, the rowleyite crystal investigated
344 by single-crystal X-ray diffraction likely remained intact during acquisition of the X-ray intensity
345 data (no degradation of the crystal was evidenced experimentally). Using the observed weight
346 fractions of the channel constituents (NH_4, K, Na, Cl) from electron-microprobe analysis, we
347 calculated atomic proportions and then scaled the result to give a total 8.64+ charge to balance
348 the 8.64– framework charge. This gives $(NH_4)_{8.24}Na_{3.31}K_{2.41}Cl_{5.32}$ *pfu* ; however, the Cl content is

Always consult and cite the final, published document. See http:/www.minsocam.org or GeoscienceWorld

somewhat low in comparison to the minimal Cl value of $Cl_{6.29}$ *pfu* inferred from the structure (Cl content at the *X* sites is unknown). We adjusted the wt% Cl to conform with $Cl_{6.29}$ and then applied a slight proportional increase to the (NH_4, K, Na) values, preserving the 8.64+ *pfu* charge. The electron scattering difference between *total refined channel scattering* (498 *e*) and *scaled channel constituents from EMPA* (370 *e*, excluding H), is consistent with approximately 16 H_2O *pfu*. This result derived from the combination of structure refinement (*i.e.* framework V^{5+}/V^{4+} and P/As; and total channel electrons) and electron-microprobe (approximate channel constituent proportioning) appears in the 2nd column of Table 2. Relative to the measured index of refraction of 1.70, this result gives a Gladstone-Dale calculated value of 1.62, suggesting that unaccounted channel content remains. We attribute this 'missing' channel component to: (i) instability of rowleyite during sample preparation and analysis by electron-microprobe and (ii) highly disordered and mobile channel occupation during X-ray diffraction measurement. For comparison in Table 2, we have included rowleyite chemical models that contain increased channel constituents: (i) column 3 includes double the amount of H_2O; (ii) column 4 includes 10% additional (NH_4, K, Na) and 50% more H_2O, with additional Cl to charge balance. Both scenarios (column 3 and 4) represent plausible adaptations to the observed analytical data, and give calculated index of refraction values in closer agreement with that observed, while scenario 4 has the additional advantage that it provides a calculated density matching the measured density. Given the complexities in ascertaining the true total channel composition in rowleyite experimentally, we think it most prudent to define rowleyite with emphasis placed upon the ordered components. The framework contains V^{5+} dominant over V^{4+} and P dominant over As, and minor oxidation differences during crystallization are likely to yield varying V^{5+}/V^{4+} ratios

Always consult and cite the final, published document. See http:/www.minsocam.org or GeoscienceWorld

371 which will couple to variations in charged channel constituents. The following chemical formula
372 encompasses these aspects: $[Na(NH_4,K)_9Cl_4][V^{5+,4+}{}_2(P,As)O_8]_6 \cdot n[H_2O,Na,NH_4,K,Cl]$.
373

374 ## IMPLICATIONS

375 In recent years, there has been a great deal of research focusing on the design of POM
376 frameworks because of their potential technological uses related, in particular, to their
377 mesoporosity and catalytic activity, electronic and ionic transport, ferro- or ferrimagnetism, and
378 photoluminescence. Queen et al. (2010) reported on the first family of salt-inclusion solids (SISs)
379 with mesoporous frameworks comprised of interlinked POV clusters. One of these,
380 $Cs_{3.64}Na_{1.40}(V_4O_8)(AsO_4)_2Cl_{3.04}$, has a $[V^{5+}{}_2AsO_8]$ framework that is essentially the same as the
381 $[V^{5+,4+}{}_2(P,As)O_8]$ framework in rowleyite. Queen et al. noted that the use of salts as templates
382 allowed the creation of porous materials at high temperatures (>600°C). In this respect, it is of
383 special interest to note that within the POV framework of rowleyite is a 3-D ordered
384 $[Na(NH_4,K)_9Cl_4]$ salt net. It can be presumed that this salt net served as a template for the
385 formation of the highly porous $[V^{5+,4+}{}_2(P,As)O_8]$ framework in rowleyite; however, the
386 occurrence of rowleyite in an relatively low-temperature mineral assemblage suggests that salt-
387 templating can also be a viable approach for the synthesis of porous framework structures at
388 temperatures much lower than 600°C.
389

390 ## ACKNOWLEDGEMENTS

391 Reviewers xxx and yyy are thanked for constructive comments, which improved the
392 manuscript. Frank Hawthorne is thanked for providing use of the X-ray diffractometer at the
393 University of Manitoba for collection of the structure data. Keith Wentz, claim holder of the

Always consult and cite the final, published document. See http:/www.minsocam.org or GeoscienceWorld

Rowley mine, is thanked for allowing underground access for the study of the occurrence and the collecting of specimens. This study was funded, in part, by the John Jago Trelawney Endowment to the Mineral Sciences Department of the Natural History Museum of Los Angeles County.

REFERENCES

Baerlocher, C., McCusker, L.B., and Olson, D.H. (2007) *Atlas of Zeolite Framework Types*, 6th Edition. Elsevier Science, 404 p.

Bastin, G.F., and Heijligers, H.J.M. (1991) Quantitative electron probe microanalysis of nitrogen. Scanning, 13, 325-342.

Bojar, H.-P., Walter, F., Baumgartner, J., and Färber, G. (2010) Ammineite, $CuCl_2(NH_3)_2$, a new species containing an ammine complex: mineral data and crystal structure. Canadian Mineralogist, 48, 1359-1371.

Brese, N.E., and O'Keeffe, M. (1991) Bond-valence parameters for solids. Acta Crystallographica, B47, 192-197.

Chukanov, N.V., Aksenov, S.M., Rastsvetaeva, R.K., Lyssenko, K.A., Belakovskiy, D.I., Färber, G., Möhn, G., and Van, K.V. (2015) Antipinite, $KNa_3Cu_2(C_2O_4)_4$, a new mineral species from a guano deposit at Pabellón de Pica, Chile. Mineralogical Magazine, 79, 1111-1121.

Des Marais, D.J., Mitchell, J.M., Meinschein, W.G., and Hayes, J.M. (1980) The carbon isotope biogeochemistry of the individual hydrocarbons in bat guano and the ecology of the insectivorous bats in the region of Carlsbad, New Mexico. Geochimica et Cosmochimica Acta, 44, 2075-2086.

Always consult and cite the final, published document. See http:/www.minsocam.org or GeoscienceWorld

415 Fleming, T. H., Nuñez R.A., and Sternberg, L.S.L. (1993) Seasonal changes in the diets of
416 migrant and non-migrant nectarivorous bats as revealed by carbon stable isotope analysis.
417 Oecologia 94, 72-75.
418 Frost, R.L, Locke, A., and Martens, W.N. (2008) Synthesis and Raman spectroscopic
419 characterization of the oxalate mineral wheatleyite $Na_2Cu^{2+}(C_2O_4)_2 \cdot 2H_2O$, Journal of Raman
420 Spectroscopy, 39, 901-908.
421 Frost, R.L., Palmer, S.J., Cejka, J., Sejkora, J., Plasil, J., Bahfenne, S., and Keeffe, E.C. (2011) A
422 Raman spectroscopic study of the different vanadate groups in solid-state compounds –
423 model case: mineral phases vesignieite $[BaCu_3(VO_4)_2(OH)_2]$ and volborthite
424 $[Cu_3V_2O_7(OH)_2 \cdot H_2O]$. Journal of Raman Spectroscopy, 42, 1701-1710.
425 Frost, R.L., Scholz, R., Belotti, F.M., Lopez, A., and Theiss, F.L. (2015) A vibrational
426 spectroscopic study of the phosphate mineral vantasselite $Al_4(PO_4)_3(OH)_3 \cdot 9H_2O$.
427 Spectrochimica Acta A – Molecular and Biomolecular Spectroscopy, 147, 185-192.
428 Frost, R.L., and Xi, Y. (2012) Vibrational spectroscopic study of the minerals cavansite and
429 pentagonite $Ca(V^{4+}O)Si_4O_{10} \cdot 4H_2O$. Spectrochimica Acta A – Molecular and Biomolecular
430 Spectroscopy, 95, 263-269.
431 Garavelli, A., Mitolo, D., Pinto, D., and hVurro, F. (2013) Lucabindiite, $(K,NH_4)As_4O_6(Cl,Br)$, a
432 new fumarole mineral from the “La Fossa” crater at Vulcano, Aeolian Islands, Italy.
433 American Mineralogist, 98, 470-477.
434 Garvie, L.A.J. (2003) Decay-induced biomineralization of the saguaro cactus (Carnegiea
435 gigantea). American Mineralogist, 88, 1879-1888.

Always consult and cite the final, published document. See http:/www.minsocam.org or GeoscienceWorld

436 Hofmann, B.A., and Bernasconi, S.M. (1998) Review of occurrences and carbon isotope
437 geochemistry of oxalate minerals: implications for the origin and fate of oxalate in diagenetic
438 and hydrothermal fluids. Chemical Geology, 149, 127-146.
439 Holleman, A.F., and Wiberg, E. (2001) Inorganic Chemistry. Academic Press, 613 p.
440 Kampf, A.R., Nash, B.P., and Loomis, T.A. (2013) Phosphovanadylite-Ca,
441 $Ca[V^{4+}_4P_2O_8(OH)_8]\cdot 12H_2O$, the Ca analogue of phosphovanadylite-Ba. American
442 Mineralogist, 97, 439-443.
443 Malinovskii, A., Pobedimskaya, E.A., and Belov, N.V. (1976) Crystal structure of traskite. Soviet
444 Physics Doklady, 21, 426-428.
445 Mandarino, J.A. (2007) The Gladstone–Dale compatibility of minerals and its use in selecting
446 mineral species for further study. Canadian Mineralogist, 45, 1307-1324.
447 Mercè Bergadà, M, Villaverde, V., and Román, D. (2013) Microstratigraphy of the Magdalenian
448 sequence at Cendres Cave (Teulada-Moraira, Alicante, Spain): Formation and diagenesis.
449 Quaternary International, 315, 56-75.
450 O'Leary, M.H. (1988) Carbon isotopes in photosynthesis. BioScience, 38, 325-326.
451 Pankewitz, T., Lagutschenkov, A., Niedner-Schatteburg, G., Xantheas, S.S., and Lee, Y.T.
452 (2007) Infrared spectrum of $NH_4^+(H_2O)$: Evidence for mode specific fragmentation. Journal
453 of Chemical Physics, 126, 074307.
454 Pouchou, J.-L., and Pichoir, F. (1991) Quantitative analysis of homogeneous or stratified
455 microvolumes applying the model "PAP." In: Heinrich, K.F.J., and Newbury, D.E. (eds)
456 Electron Probe Quantitation. Plenum Press, New York, pp. 3l-75.
457 Queen, W.L., Hwu, S., and Reighard, S. (2010) Salt-templated mesoporous solids comprised of
458 interlinked polyoxovanadate clusters. Inorganic Chemistry, 49, 1316-1318.

Always consult and cite the final, published document. See http:/www.minsocam.org or GeoscienceWorld

Rivera, E.R., and Smith, B.N. (1979) Crystal morphology and ^{13}Carbon/^{12}Carbon composition of solid oxalate in cacti. Plant Physiology, 64, 966-970.

Shannon, R.D. (1976) Revised Effective Ionic Radii and Systematic Studies of Interatomie Distances in Halides and Chaleogenides.

Sheldrick, G.M. (2015) Crystal structure refinement with SHELXL. Acta Crystallographica, C71, 3-8.

Schindler, M., Hawthorne, F.C., Baur, W.H. (2000): Crystal chemical aspects of vanadium: polyhedral geometries, characteristic bond valences, and polymerization of (VO_n) polyhedra. Chemistry of Materials, 12, 1248-1259.

Snow, M.R., Pring, A., and Allen, N. (2014) Minerals of the Wooltana Cave, Flinders Ranges, South Australia. Transactions of the Royal Society of South Australia, 138, 214-230.

Thorpe, T.E. (1922) A Dictionary of Applied Chemistry, Volume 3. Longmans, Green, and Company, London, 735 p.

Varriale, L., Bhalla, N., Tonge, N.M., Ellis, A.M., and Wright, T.G. (2011) Near-infrared spectroscopy of $LiNH_3$: First observation of electronic spectrum. Journal of Chemical Physics, 134, 124304.

Von Wagner, R. (1900) Manual of Chemical Technology, translated and edited by W. Crookes. Appleton and Company, New York, 968 p.

Wilson, W.E., and D.K. Miller (1974) Minerals of the Rowley mine, Mineralogical Record, 5, 10-30.

Wurster, C.M., McFarlane, D.A., and Bird, M.I. (2007) Spatial and temporal expression of vegetation and atmospheric variability from stable carbon and nitrogen isotope analysis of bat guano in the southern United States. Geochimica et Cosmochimica Acta, 71, 3302-3310.

Always consult and cite the final, published document. See http:/www.minsocam.org or GeoscienceWorld

482 Zheng, N., Bu, X., Wang, B., and Feng, P. (2002) Microporous and photoluminescent
483 chalcogenide zeolite analogs. Science, 298, 2366-2369.

484

Always consult and cite the final, published document. See http:/www.minsocam.org or GeoscienceWorld

485 FIGURE CAPTIONS

486 Figure 1. Rowleyite crystals (black) on mottramite (olive green) and quartz; FOV 0.56 mm
487 across.

488

489 Figure 2. Raman spectrum of rowleyite.

490

491 Figure 3. Infra-red spectrum of rowleyite.

492

493 Figure 4. The rowleyite $[A_9Cl_4]^{5+}$ salt cluster coordinated by four Na atoms.

494

495 Figure 5. (a) Ball and stick representation of $[V_4O_{16}]$ unit in rowleyite with short vanadyl bond
496 shown as thick stick. (b) Polyhedral representation of $[V_4O_{16}]$ unit with attached PO_4 tetrahedra
497 in rowleyite.

498

499 Figure 6. The rowleyite structure, (a) viewed slightly canted down [110] with [001] vertical and
500 (b) viewed down [111]. The salt cluster centered at (1/8,1/8,1/8) is shown in black and linking Na
501 atoms are shown in yellow. To more clearly show all of the components of the framework, the
502 salt clusters and linking Na atoms have been omitted in the lower right portion of each projection.
503 Note that the *X* sites contained within the large open channels are not shown.

504

505 Figure 7. Cages within the rowleyite framework. Small cages (red) centered at 1/8, 1/8, 1/8 host
506 the $[A_9Cl_4]^{5+}$ salt cluster. Large cages (grey) centered at 3/8, 3/8, 3/8 host the *X* sites.

Always consult and cite the final, published document. See http:/www.minsocam.org or GeoscienceWorld

507 Table 1. Analytical results for rowleyite.

Constituent	Mean	Range	S.D.	Probe Standard
$(NH_4)_2O$	9.47	8.56–10.72	0.84	syn. AIN
Na_2O	4.53	3.91–5.26	0.52	albite
K_2O	5.00	4.72–5.18	0.18	sanidine
P_2O_5	19.28	18.99–19.63	0.25	apatite
V_2O_5	42.23	41.01–44.22	1.23	syn. YVO_4
As_2O_5	4.07	3.94–4.25	0.13	syn. GaAs
Cl	8.32	7.78–8.96	0.46	tugtupite

508 See Table 2 for complete analyses based on a combination of EPMA and structural evidence.
509

510 Table 2. Chemical data for rowleyite with different hypothetical channel constituents.
511

	1	2	3	4
	EMPA	SREF + EMPA	SREF + EMPA	Column 2
		(16 H_2O)	(32 H_2O)	+ 10% (NH_4,Na,K)
wt%				+ 50% (H_2O)
V_2O_5	42.23	34.75	31.09	31.76
VO_2		8.94	8.00	8.17
P_2O_5	19.28	15.30	13.69	13.98
As_2O_5	4.07	3.38	3.02	3.09
$(NH_4)_2O$	9.47	9.37	8.38	9.41
Na_2O	4.53	4.48	4.01	4.50
K_2O	5.00	4.96	4.44	4.99
Cl	8.32	9.11	8.15	10.29
H_2O		11.77	21.06	16.13
O=Cl		-2.06	-1.84	-2.32
Total		100	100	100
apfu				
V^{5+}		9.36	9.36	9.36
V^{4+}		2.64	2.64	2.64
P^{5+}		5.28	5.28	5.28
As^{5+}		0.72	0.72	0.72
$(NH_4)^+$		8.81	8.81	9.69
Na^+		3.54	3.54	3.89
K^+		2.58	2.58	2.84
Cl^-		6.29	6.29	7.78
H_2O		16	32	24
$1 - (K_p/K_c)$		-0.166 (poor)	-0.029 (excellent)	-0.055 (good)
$Density_{calc}$ ($g \cdot cm^{-3}$)		2.042	2.282	2.234

512

Always consult and cite the final, published document. See http:/www.minsocam.org or GeoscienceWorld

513 Table 3. Powder X-ray diffraction data (d in Å) for rowleyite.

I_{obs}	d_{obs}	d_{calc}	I_{calc}	hkl
26	18.4	18.3043	49	1 1 1
70	11.3	11.2091	100	2 2 0
31	9.6	9.5591	31	3 1 1
		9.1522	1	2 2 2
63	7.97	7.9260	63	4 0 0
24	7.29	7.2734	34	3 3 1
13	6.49	6.4716	18	4 2 2
16	6.11	6.1014	13	3 3 3
9	5.39	5.3590	7	5 3 1
30	5.05	5.0128	7	6 2 0
		4.8348	1	5 3 3
15	4.611	4.5761	8	4 4 4
28	4.454	4.4394	20	7 1 1
23	4.215	4.2366	1	6 4 2
		4.1275	1	7 3 1
13	3.980	3.9630	7	8 0 0
8	3.902	3.8733	3	7 3 3
5	3.688	3.6609	5	7 5 1
12	3.545	3.5446	1	8 4 0
		3.4800	1	7 5 3
19	3.336	3.3797	3	6 6 4
		3.3235	3	9 3 1
65	3.216	3.2358	4	8 4 4
		3.1864	32	7 7 1
31	3.127	3.1088	12	8 6 2
		3.0649	8	9 5 1
15	2.969	2.9564	2	9 5 3
17	2.880	2.8942	3	10 4 2
100	2.811	2.8023	74	8 8 0
22	2.701	2.7700	20	9 7 1
		2.7186	7	8 6 6
16	2.661	2.6891	3	11 3 3
		2.6420	7	8 8 4
14	2.593	2.6149	2	11 5 1
		2.5715	1	12 2 2
14	2.519	2.5064	5	12 4 0
		2.4832	1	9 9 1
4	2.436	2.4460	1	10 8 2
		2.4245	6	11 7 1
4	2.384	2.3697	5	11 7 3
12	2.299	2.2880	1	8 8 8
		2.2704	1	13 5 1
9	2.223	2.2418	2	10 10 0
		2.2252	1	11 9 1
		2.1983	1	12 8 0
9	2.1556	2.1572	6	12 6 6
		2.1424	2	11 7 7
34	2.1112	2.1183	5	12 8 4
		2.1043	6	15 1 1
7	2.0378	2.0338	3	11 11 1
		2.0132	3	12 10 2
		2.0011	1	13 9 1
12	1.9867	1.9815	9	16 0 0
12	1.9580	1.9512	11	14 8 2
34	1.9319	1.9223	1	12 8 8
		1.9118	1	15 7 1
		1.8947	1	12 10 6
14	1.8742	1.8846	1	15 7 3
		1.8682	3	12 12 0
12	1.8442	1.8585	3	11 11 7
		1.8428	2	14 10 0
		1.8335	1	17 3 1
18	1.7826	1.8094	2	17 3 3
		1.7863	1	17 5 1
		1.7641	2	15 7 7
		1.7506	1	16 6 6
		1.7219	1	13 11 7
		1.7094	2	14 12 2
19	1.6912	1.7020	1	15 11 1
		1.6898	9	12 12 8
		1.6827	3	15 9 7
31	1.6517	1.6709	5	16 10 2
		1.6640	1	19 1 1
		1.6460	1	17 9 1
		1.6350	1	18 6 4
16	1.6190	1.6285	1	17 9 3
		1.6179	7	16 8 8
		1.6116	3	19 5 1
		1.6013	2	16 10 6
6	1.5890	1.5952	3	17 9 5
		1.5852	3	20 0 0

514

515

Always consult and cite the final, published document. See http:/www.minsocam.org or GeoscienceWorld

Table 4. Data collection and structure refinement details for rowleyite.

Diffractometer	Bruker D8 three-circle; multilayer optics; APEX-II CCD
X-ray radiation / source	Mo$K\alpha$ (λ = 0.71073 Å) / rotating anode
Temperature	293(2) K
Structural Formula	$[(NH_4)_{6.74}K_{2.26}Cl_4][(V_{12}P_{5.28}As_{0.72}O_{48}]\cdot(NH_4)_{41.39}Na_{1.08}Cl_{2.23}$
Space group	*Fd*-3*m*
Unit cell dimensions	a = 31.704(14) Å
V	31867(42) Å^3
Z	16
Density (for above formula)	2.17 g cm^{-3}
Absorption coefficient	2.20 mm^{-1}
F(000)	23250
Crystal size	25 × 20 × 4 μm
θ range	2.13 to 27.49°
Index ranges	$-41 \le h \le 41$, $-41 \le k \le 41$, $-41 \le l \le 41$
Refls collected / unique	70994 / 1770; R_{int} = 0.138
Reflections with $F_o > 4\sigma F$	1218
Completeness to θ = 27.49°	99.9%
Max. and min. transmission	0.991 and 0.947
Refinement method	Full-matrix least-squares on F^2
Parameters / restraints	160 / 0
GoF	1.032
Final R indices [$F_o > 4\sigma F$]	R_1 = 0.0400, wR_2 = 0.1032
R indices (all data)	R_1 = 0.0677, wR_2 = 0.1201
Largest diff. peak / hole	+0.52 / –0.48 e/A^3

*$R_{int} = \Sigma|F_o^2\text{-}F_o^2(\text{mean})|/\Sigma[F_o^2]$. GoF = $S = \{\Sigma[w(F_o^2-F_c^2)^2]/(n-p)\}^{1/2}$. $R_1 = \Sigma||F_o|\text{-}|F_c||/\Sigma|F_o|$. $wR_2 = \{\Sigma[w(F_o^2-F_c^2)^2]/\Sigma[w(F_o^2)^2]\}^{1/2}$; $w = 1/[\sigma^2(F_o^2) + (aP)^2 + bP]$ where a is 0.056, b is 472 and P is $[2F_c^2 + \text{Max}(F_o^2,0)]/3$.

Always consult and cite the final, published document. See http:/www.minsocam.org or GeoscienceWorld

Table 5. Atom coordinates and displacement parameters (Å^2) for rowleyite.

	Occ.	*x*/*a*	*y*/*b*	*z*/*c*	U_{eq}/U_{iso}	U^{11}	U^{22}	U^{33}	U^{23}	U^{13}	U^{12}
V1	1	0.33174(3)	0.07076(2)	0.07076(2)	0.0151(2)	0.0189(5)	0.0132(3)	0.0132(3)	0.0019(3)	0.0010(2)	0.0010(2)
V2	1	0.33163(3)	0.17757(2)	0.07243(2)	0.0145(2)	0.0168(4)	0.0134(3)	0.0134(3)	0.0001(3)	0.0009(2)	-0.0009(2)
P/As	0.880/0.120(4)	0.37518(2)	0.12482(2)	0	0.0133(3)	0.0142(4)	0.0142(4)	0.0114(5)	0.0018(3)	0.0018(3)	0.0000(5)
O1	1	0.37541(9)	0.16469(7)	0.02906(7)	0.0179(5)	0.0200(12)	0.0175(12)	0.0162(11)	0.0006(9)	0.0023(11)	-0.0018(12)
O2	1	0.37495(9)	0.08414(7)	0.02705(8)	0.0196(5)	0.0198(12)	0.0195(12)	0.0196(12)	0.0028(9)	0.0048(12)	0.0013(12)
O3	1	0.31158(7)	0.12438(8)	0.06488(7)	0.0164(5)	0.0178(11)	0.0143(11)	0.0170(12)	0.0006(10)	0.0009(9)	-0.0009(10)
O4	1	0.29787(13)	0.04376(8)	0.04376(8)	0.0259(9)	0.031(2)	0.0232(13)	0.0232(13)	-0.0031(17)	-0.0002(12)	-0.0002(12)
O5	1	0.29835(12)	0.20441(8)	0.04559(8)	0.0214(8)	0.025(2)	0.0194(12)	0.0194(12)	0.0026(15)	-0.0014(11)	0.0014(11)
Na	1.08(2)	0.25	0.25	0	0.0238(17)	0.0238(17)	0.0238(17)	0.0238(17)	-0.0037(12)	-0.0037(12)	0.0037(12)
N1/K1	0.748/0.252(10)	0.24853(8)	0.12237(12)	0.00147(8)	0.0453(15)	0.0341(15)	0.068(3)	0.0341(15)	0.0090(13)	-0.0065(13)	-0.0090(13)
N2/K2	0.753/0.247(13)	0.23666(15)	0.125	0.125	0.0382(18)	0.041(3)	0.037(2)	0.037(2)	-0.004(2)	0	0
Cl1	0.977(11)	0.19256(5)	0.19256(5)	0.05744(5)	0.0327(10)	0.0327(10)	0.0327(10)	0.0327(10)	-0.0020(7)	-0.0020(7)	0.0020(7)
Cl2	0.989(11)	0.18890(5)	0.06110(5)	0.06110(5)	0.0331(9)	0.0331(9)	0.0331(9)	0.0331(9)	0.0051(7)	-0.0051(7)	-0.0051(7)
Cl3	0.765(12)	0.39002(13)	0.125	0.125	0.0419(13)	0.050(3)	0.0376(12)	0.0376(12)	0.0048(14)	0	0
X1	1.23(3)	0.4587(3)	0.1927(2)	0.0573(2)	0.126(5)	0.071(6)	0.154(7)	0.154(7)	-0.046(7)	-0.019(5)	0.019(5)
X2	0.42(4)	0.3752(6)	-0.0552(5)	-0.0552(5)	0.066(9)	0.055(12)	0.071(11)	0.071(11)	0.042(10)	0.024(8)	0.024(8)
X3	1.30(8)	0.4569(11)	0.0486(16)	0.0486(16)	0.79(6)	0.22(3)	1.07(9)	1.07(9)	0.88(9)	0.24(4)	0.24(4)
X4	0.55(4)	0.4194(7)	0.0225(4)	0.0225(4)	0.085(10)	0.119(17)	0.067(9)	0.067(9)	0.034(9)	0.050(9)	0.050(9)
X5	0.91(5)	0.3741(8)	-0.0134(6)	-0.0134(6)	0.248(19)	0.25(3)	0.25(2)	0.25(2)	0.00(2)	0.052(16)	0.052(16)
X6	0.32(3)	0.4210(8)	0.125	0.125	0.039(10)	0.014(16)	0.052(12)	0.052(12)	0.010(14)	0	0
X7	0.30(3)	0.4413(6)	0.1006(6)	0.1006(6)	0.063(11)	0.014(11)	0.088(15)	0.088(15)	-0.005(15)	0.004(7)	0.004(7)
X8	0.83(6)	0.381(6)	-0.0535(11)	-0.099(6)	0.66(14)	1.0(4)	0.43(4)	0.53(12)	0.18(6)	-0.26(15)	0.13(6)
X9	0.42(4)	0.2630(10)	-0.0130(10)	-0.0130(10)	0.11(2)	0.11(2)	0.11(2)	0.11(2)	0.10(2)	-0.10(2)	-0.10(2)
X10	0.29(6)	0.4142(9)	-0.0858(9)	-0.0858(9)	0.07(2)	0.07(2)	0.07(2)	0.07(2)	0.003(16)	0.003(16)	0.003(16)
X11	0.10(3)	0.375	-0.104(2)	-0.125	0.04(3)	0.04(3)	0.03(4)	0.04(3)	0	0.00(3)	0
X12	0.09(3)	0.4364(17)	0.0692(12)	0.0692(12)	0.018(19)						

Always consult and cite the final, published document. See http:/www.minsocam.org or GeoscienceWorld

575 Table 6. Selected bond distances in rowleyite.

V1–O2 (×2)	1.994(3)	Na–O5 (×6)	2.555(4)
V1–O3 (×2)	1.826(3)	Na–Cl1 (×2)	3.154(3)
V1–O4	1.618(4)	<Na–φ>	2.705
V1–Cl3	3.054(3)		
		*A*1–O1 (×2)	2.917(4)
V2–O1 (×2)	1.996(3)	*A*1–O3 (×2)	2.836(3)
V2–O3 (×2)	1.818(3)	*A*1–O4 (×2)	3.234(4)
V2–O5	1.601(4)	*A*1–O5	3.281(5)
V2–Cl3	2.997(3)	*A*1–O5 (×2)	3.349(4)
		*A*1–Cl1	3.354(4)
P–O1 (×2)	1.564(3)	*A*1–Cl2	3.305(4)
P–O2 (×2)	1.549(3)	<*A*1–φ>	3.147
<P–O>	1.557		
		*A*2–O3 (×4)	3.046(5)
X–*X* channel close approaches		*A*2–Cl1 (×2)	3.336(3)
*X*2–*X*5	1.87(3)	*A*2–Cl2 (×2)	3.241(3)
*X*2–*X*8	1.4(2)	<*A*2–φ>	3.167
*X*2–*X*8	2.2(3)		
*X*2–*X*10	1.85(2)	O–*X* approaches	
*X*3–*X*4	1.67(6)	O1–*X*1	2.927(4)
*X*3–*X*12	1.13(7)	O2–*X*3	2.91(3)
*X*4–*X*5	2.16(4)	O2–*X*4	2.414(3)
*X*4–*X*12	2.16(6)	O2–*X*5	3.35(3)
*X*6–*X*7	1.27(3)	O2–*X*7	3.18(2)
*X*7–*X*7	2.19(6)	O2–*X*12	2.41(4)
*X*7–*X*12	1.42(6)	O4–*X*1	3.219(9)
*X*8–*X*8	0.9(6)	O4–*X*9	2.77(3)
*X*8–*X*8	1.45(9)		
*X*8–*X*8	1.7(3)	Cl–*X* close approaches	
*X*8–*X*8	2.0(3)	Cl3–*X*6	0.98(2)
*X*8–*X*10	1.53(10)	Cl3–*X*7	1.96(2)
*X*8–*X*11	1.83(10)		
*X*11–*X*11	0.92(10)		
*X*11–*X*11	1.30(15)		

576

577

Always consult and cite the final, published document. See http:/www.minsocam.org or GeoscienceWorld

This is a preprint, the final version is subject to change, of the American Mineralogist (MSA)
Cite as Authors (Year) Title. American Mineralogist, in press.
(DOI will not work until issue is live.) DOI: http://dx.doi.org/10.2138/am-2017-5977

Table 7. Site assignments for rowleyite (*epfu* / *apfu* with $Z = 16$).

Site	Mult.[1]	SREF[2]	V	P	As	Na	NH_4	K	Cl	□	*epfu*[3]
V1	96g	138	6								138
V2	96g	138	6								138
P	96h	103.0(5)		5.28	0.72						103.0
Na	16c	11.9(3)				1					11
*A*1	96g	60.1(8)					4.49	1.51			60.1
*A*2	48f	29.9(5)					2.26	0.74			29.9
Cl1	32e	33.2(4)							2		34
Cl2	32e	33.6(4)							2		34
Cl3	48f	39.0(6)							2.29	0.71	38.9
*X*1	96g	51.8(1.2)									
*X*2	96g	17.6(1.7)									
*X*3	96g	55(3)									
*X*4	96g	22.9(1.5)									
*X*5	96g	38(3)									
*X*6	48f	6.7(8)									
*X*7	96g	12.6(1.2)				$\Sigma = 290.3$ *epfu*					
*X*8	192i	70(5)									
*X*9	32e	5.9(5)									
*X*10	32e	4.0(9)									
*X*11	48f	2.1(6)									
*X*12	96g	3.7(1.1)									
Σ			12	6		1	6.75	2.25	6.29	0.71	

[1] site multiplicity
[2] refined site-scattering (electrons per formula unit)
[3] assigned electrons per formula unit

Always consult and cite the final, published document. See http:/www.minsocam.org or GeoscienceWorld

Table 8. Bond valence analysis for the ordered sites in rowleyite. Values are in valence units (*vu*).

	V1[1]	V2[1]	P[2]	Na	*A*1[3]	*A*2[3]	Σ
O1		$0.59^{\times 2\downarrow}$	$1.19^{\times 2\downarrow}$		$0.12^{\times 2\downarrow}$		1.90
O2	$0.59^{\times 2\downarrow}$		$1.24^{\times 2\downarrow}$				1.83
O3	$0.93^{\times 2\downarrow}$	$0.95^{\times 2\downarrow}$			$0.15^{\times 2\downarrow}$	$0.08^{\times 4\downarrow}$	2.11
O4	1.63				$0.05^{\times 2\downarrow\rightarrow}$		1.73
O5		1.71		$0.13^{\times 6\downarrow}$	0.04 $0.04^{\times 2\downarrow\rightarrow}$		1.96
Cl1				$0.07^{\times 2\downarrow}$	$0.10^{\times 3\downarrow\rightarrow}$	$0.14^{\times 2\downarrow \times 3\rightarrow}$	0.79
Cl2					$0.04^{\times 3\rightarrow}$	$0.11^{\times 2\downarrow \times 3\rightarrow}$	0.45
Cl3	$0.09^{\times 2\rightarrow}$	$0.10^{\times 2\rightarrow}$					0.38
Σ	4.76	4.89	4.86	0.92	0.90	0.82	

Bond-valence parameters are from Brese and O'Keeffe (1991).
[1] using $(V^{5+}_{0.8}V^{4+}_{0.2})$
[2] using $(P_{0.88}As_{0.12})$
[3] using K

Always consult and cite the final, published document. See http:/www.minsocam.org or GeoscienceWorld

This is a preprint, the final version is subject to change, of the American Mineralogist (MSA)
Cite as Authors (Year) Title. American Mineralogist, in press.
(DOI will not work until issue is live.) DOI: http://dx.doi.org/10.2138/am-2017-5977

Figure 1

Always consult and cite the final, published document. See http:/www.minsocam.org or GeoscienceWorld

This is a preprint, the final version is subject to change, of the American Mineralogist (MSA)
Cite as Authors (Year) Title. American Mineralogist, in press.
(DOI will not work until issue is live.) DOI: http://dx.doi.org/10.2138/am-2017-5977

Figure 2

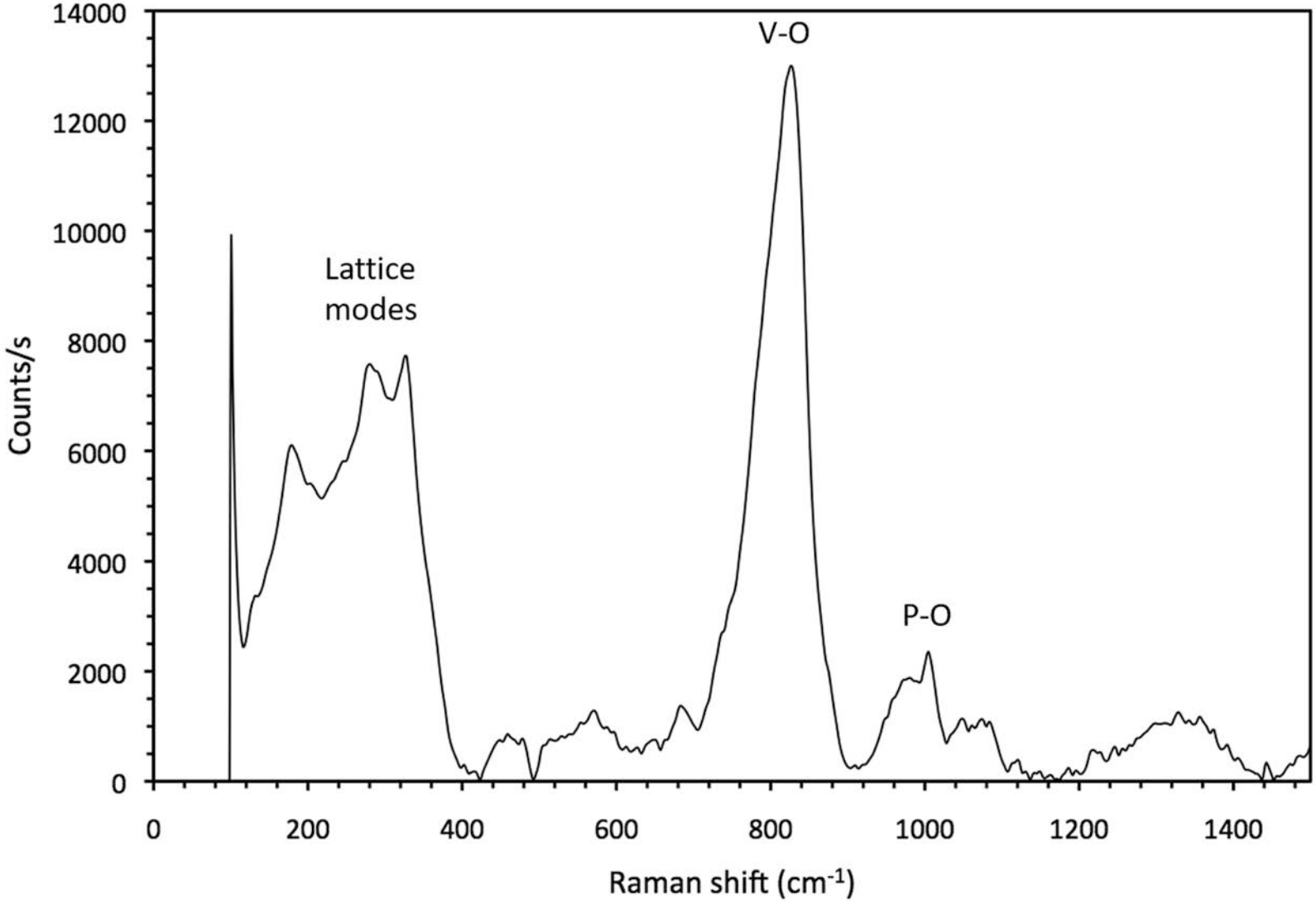

Always consult and cite the final, published document. See http:/www.minsocam.org or GeoscienceWorld

This is a preprint, the final version is subject to change, of the American Mineralogist (MSA)
Cite as Authors (Year) Title. American Mineralogist, in press.
(DOI will not work until issue is live.) DOI: http://dx.doi.org/10.2138/am-2017-5977

Figure 3

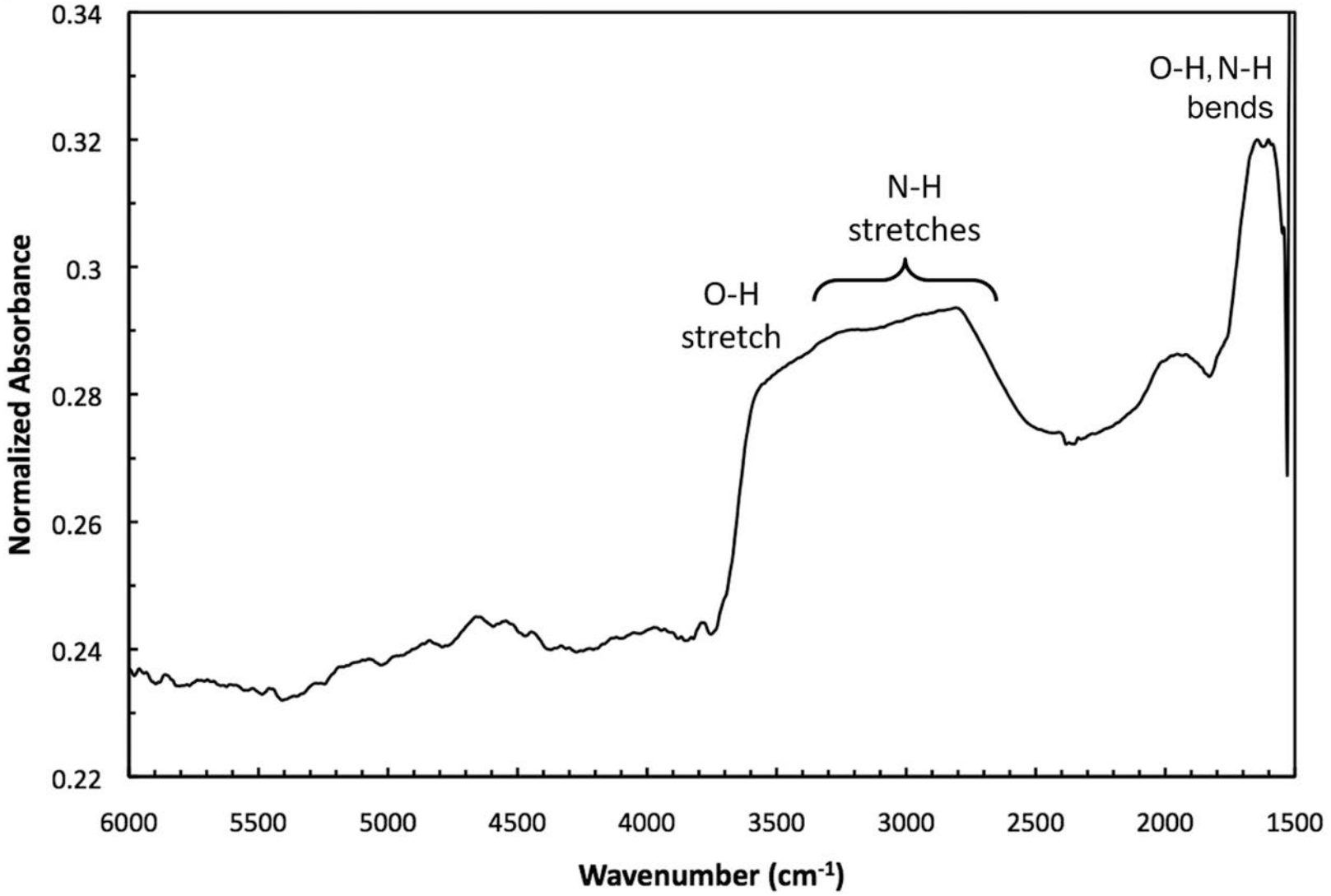

Always consult and cite the final, published document. See http:/www.minsocam.org or GeoscienceWorld

This is a preprint, the final version is subject to change, of the American Mineralogist (MSA)
Cite as Authors (Year) Title. American Mineralogist, in press.
(DOI will not work until issue is live.) DOI: http://dx.doi.org/10.2138/am-2017-5977

Figure 4

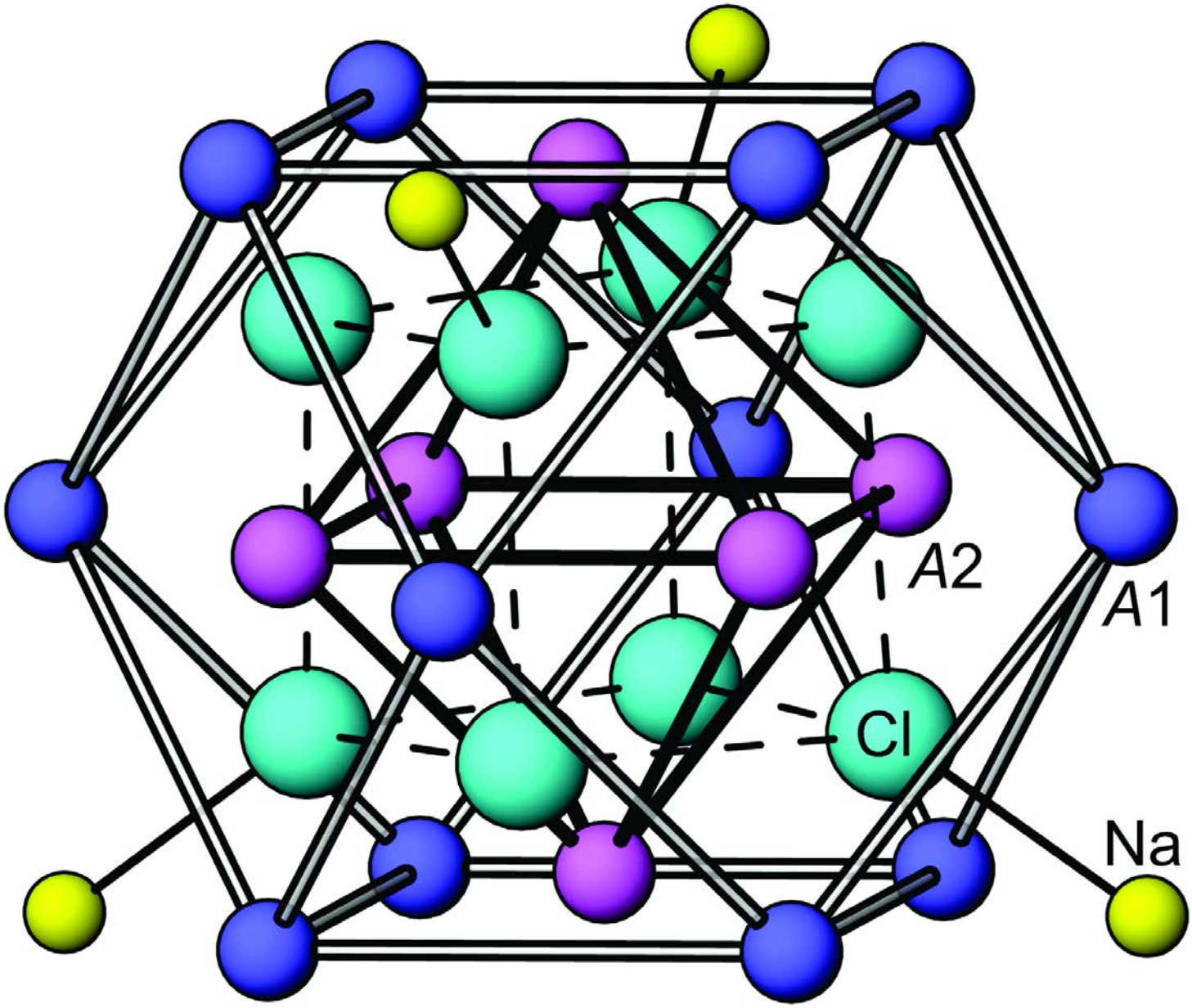

Always consult and cite the final, published document. See http:/www.minsocam.org or GeoscienceWorld

This is a preprint, the final version is subject to change, of the American Mineralogist (MSA)
Cite as Authors (Year) Title. American Mineralogist, in press.
(DOI will not work until issue is live.) DOI: http://dx.doi.org/10.2138/am-2017-5977

Figure 5

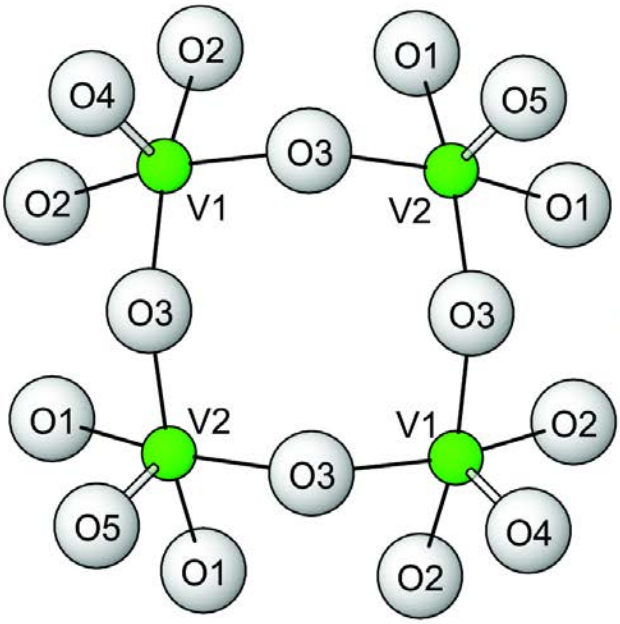

a

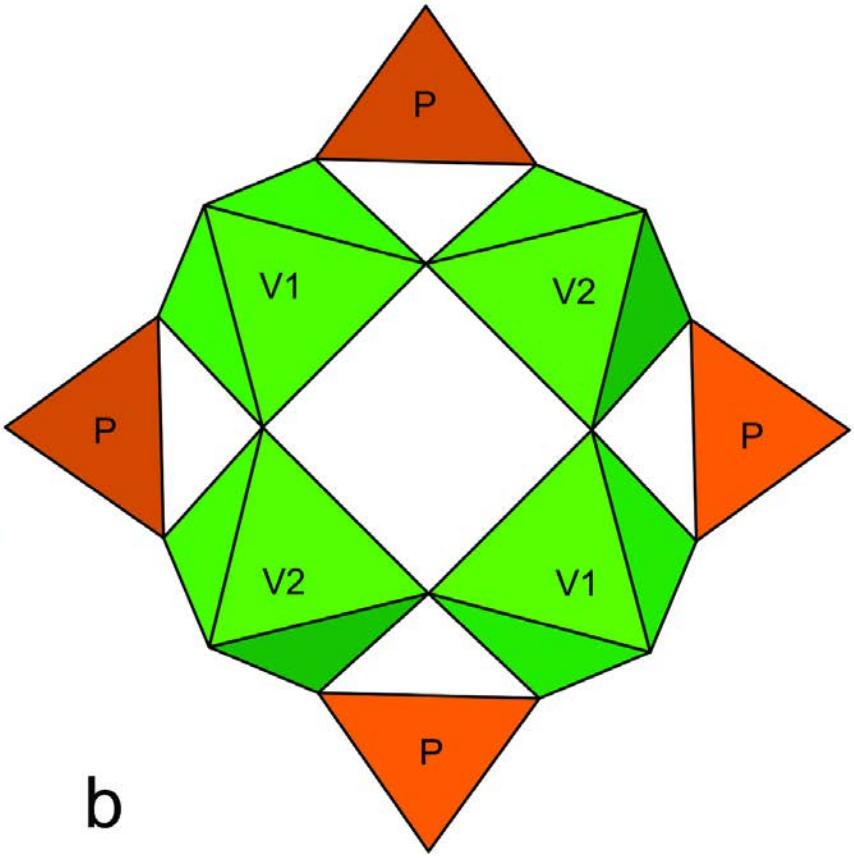

b

Always consult and cite the final, published document. See http:/www.minsocam.org or GeoscienceWorld

This is a preprint, the final version is subject to change, of the American Mineralogist (MSA)
Cite as Authors (Year) Title. American Mineralogist, in press.
(DOI will not work until issue is live.) DOI: http://dx.doi.org/10.2138/am-2017-5977

Figure 6

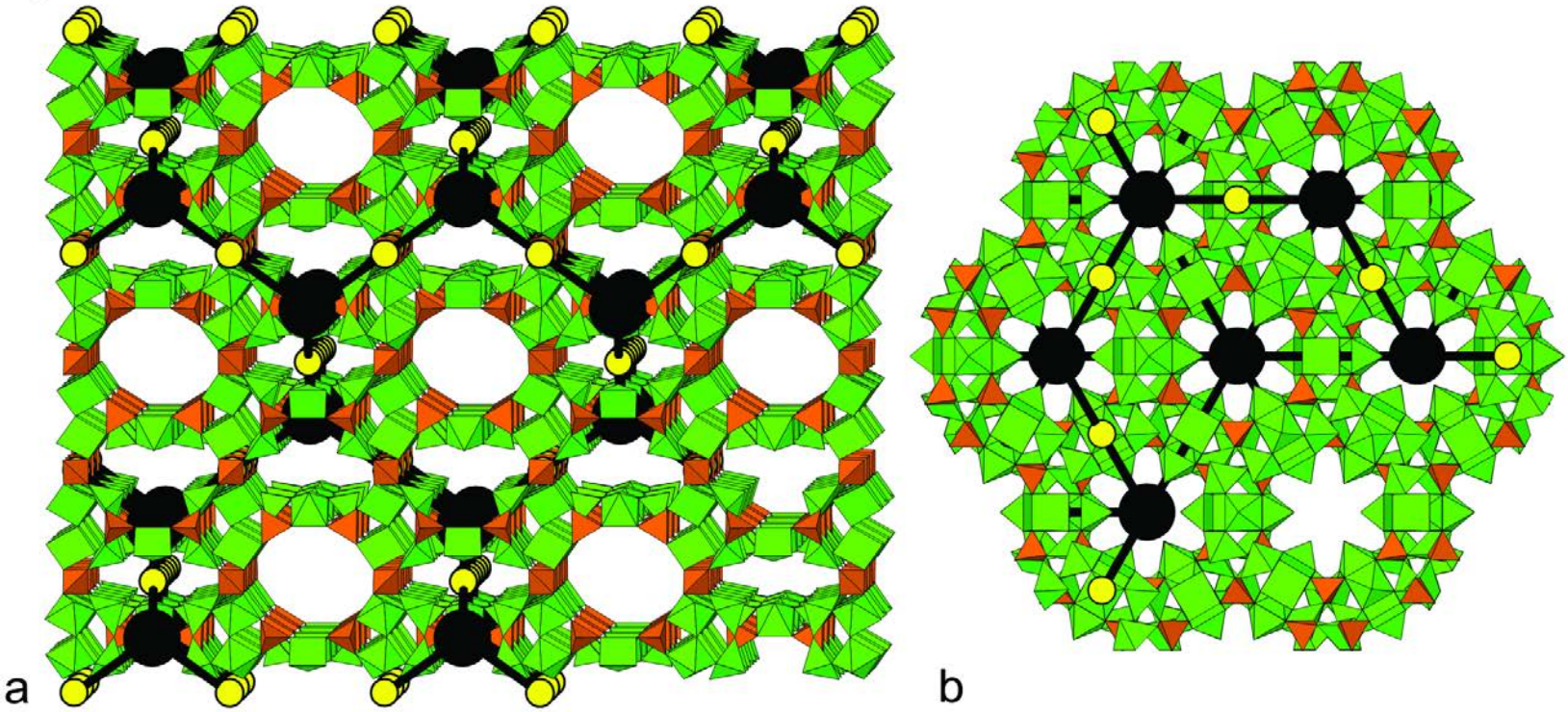

Always consult and cite the final, published document. See http:/www.minsocam.org or GeoscienceWorld

This is a preprint, the final version is subject to change, of the American Mineralogist (MSA)
Cite as Authors (Year) Title. American Mineralogist, in press.
(DOI will not work until issue is live.) DOI: http://dx.doi.org/10.2138/am-2017-5977

Figure 7

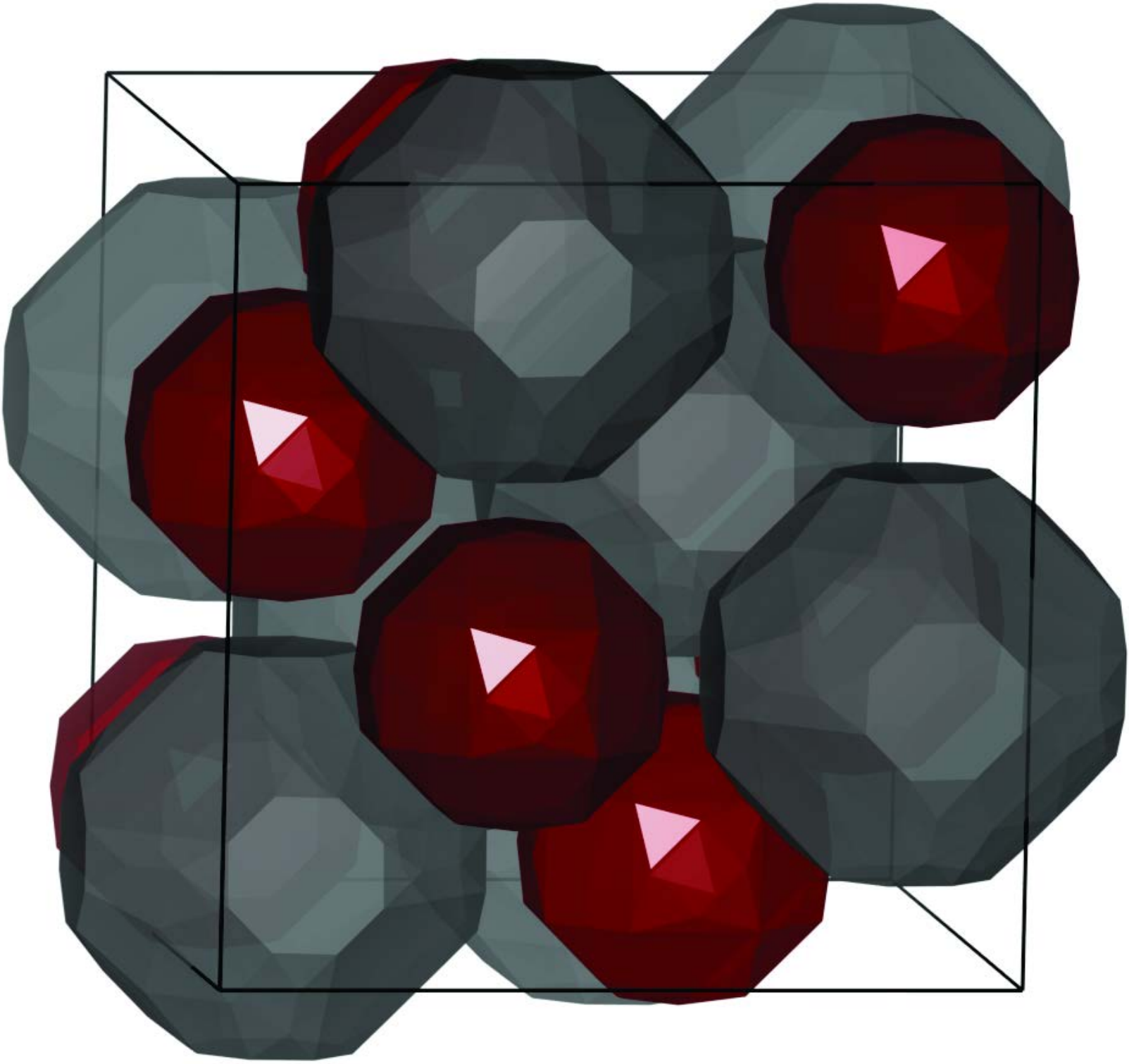

Always consult and cite the final, published document. See http:/www.minsocam.org or GeoscienceWorld